Phase transitions in Ti_5O_9 single crystals: Electrical conductivity, magnetic susceptibility, specific heat, electron paramagnetic resonance, and structural aspects

M. Marezio and D. Tranqui
Laboratoire de Cristallographie, 166 X-Centre de Tri, 38042-Grenoble Cedex, France

S. Lakkis* and C. Schlenker
Groupe des Transitions de Phases, 166 X-Centre de Tri, 38042-Grenoble Cedex, France
(Received 18 March 1976)

The physical properties of Ti_5O_9 single crystals, grown by the vapor-transport method have been studied in order to elucidate the nature of the three phases and the origin of the two successive transitions which take place as a function of temperature at ~ 130 K and ~ 140 K. Two transitions are clearly observed in the lattice-parameters, the electrical-conductivity, the magnetic-susceptibility and the specific-heat measurements. The enthalpy change of the two transitions have been found to be 135 ± 5 and 110 ± 5 cal/mole, respectively. An intense EPR line is found in the low-temperature phase and it vanishes at 130 K. No changes have been observed in the crystal structure of the three phases, as determined by the classical x-ray diffraction methods. It is suggested that $Ti^{3+}-Ti^{3+}$ pairing takes place in the low-temperature phase but that the crystal contains microdomains with unpaired Ti^{3+} cations at the domain walls which would be responsible for the strong EPR signal. The intermediate phase is proposed to be a disordered phase as far as the $Ti^{3+}-Ti^{3+}$ pairs are concerned similar to the intermediate phase of Ti_4O_7. The nature of the high-temperature phase is not clear.

I. INTRODUCTION

Most of the titanium and vanadium oxides undergo insulator-to-metal transitions as a function of temperature. Ti_5O_9 is one example of such oxides. Bartholomew and Frankl[1] showed that there are two transitions in the conductivity of Ti_5O_9 separated by 5 K at ~130 K. These authors found that at the transitions the conductivity decreased by a factor of 50 over all. They stated also that, since the conductivity of Ti_5O_9 increased with increasing temperature above the higher-temperature transition, this does not appear to be a true semiconductor to metal transition. Danley and Mulay[2] measured the magnetic susceptibility of Ti_5O_9 and found an increase of about 30% at a single transition at ~130 K.

The oxide Ti_5O_9 is a member of the homologous series Ti_nO_{2n-1}. These compounds occur as well-defined phases whose structures are related to that of rutile in that they consist of rutilelike blocks which are infinite in two dimensions and n TiO_6 octahedra in width along the third. This finite dimension is perpendicular to the $(1\bar{2}1)$ plane of the pseudorutile lattice. Along these planes, which are called crystallographic shear planes the octahedra share faces, edges, and corners, whereas inside the rutile blocks they share only edges and corners. Another idealized description of this structure is derived from that of rutile, which is schematically represented in Fig. 1. The rutile arrangement can be thought as composed of two sublattices of octahedral sites. One consists of the 000 and $\frac{1}{2}\frac{1}{2}\frac{1}{2}$ positions and the other of the $\frac{1}{2}00$ and $0\frac{1}{2}\frac{1}{2}$ ones. In the phases of the homologous series there are blocks in which the first sublattice of octahedral sites is full and adjacent blocks in which the second sublattice is full, the plane between blocks being the $(1\bar{2}1)$ of the rutile lattice. For instance, if in one block the last occupied octahedral sites are the 000 and 100 positions, in the next block the first occupied positions will be the $\frac{1}{2}0\frac{1}{2}$ instead of the 101 position. In this case the octahedra centered on the $\frac{1}{2}\frac{1}{2}\frac{1}{2}$ of one block and the other centered on the $\frac{1}{2}0\frac{1}{2}$ position of the adjacent block, share a face instead of corner.

With the exception of Ti_3O_5, the resulting structures are triclinic with n molecules per unit cell and n and $n+1$ independent cation sites for the even and odd members of the series, respectively. This crystallographic difference is due to the fact that in the odd members two cations per unit cell are in special positions, i.e., the center of symmetry. This feature seems to be responsible for the even-odd relationship which exists in most of the physi-

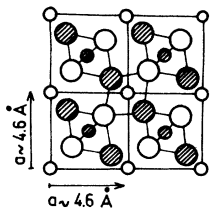

FIG. 1. Projection of four unit cells of the rutile structure perpendicular to the [001] direction. The open circles represent atoms with $z = 0$ and the full ones represent those with $z = \frac{1}{2}$.

cal and chemical properties of the phases of the homologous series Ti_nO_{2n-1} and V_nO_{2n-1}.

The insulator-to-metal transitions, which occur in Ti_4O_7, V_4O_7, V_5O_9, and in the Magnéli phases, in general, have been interpreted as transitions in which the electrons localize into covalent bonds between two transition-metal atoms so that the final spin state is a singlet. The electron localizations have been fully confirmed by the accurate determination of the crystal structures of the three phases of Ti_4O_7.[3] This compound exhibits two electrical transitions, one at 130 K and a second at 150 K. The resistivity increases abruptly at both transitions, but the large increase in magnetic susceptibility occurs only at the 150-K transition. The crystal structures as determined at 298, 140, and 120 K indicated that above 150 K the Ti cations have an average effective charge of ~3.5. Below 130 K the electrons were found to localize into alternate chains of 3+ and 4+ sites along the pseudorutile c axis, and adjacent 3+ sites paired to form metal-metal bonds. In the intermediate phase no evidence was found for charge localization. In order to rationalize these findings with the electrical and magnetic properties, it was suggested that the charge was localized into pair bonds, but there was no long-range-order correlations between bonds. In this model the lower transition is viewed as one from a state with ordered bonds to a liquid or pair bonds.[4] Heat-capacity measurements showed that a model of a disordering of the Ti^{3+} and Ti^{4+} chains would be at the unit-cell level.[5] Recent EPR data indicated that the disorder found in the intermediate phase is of dynamic type.[6]

A single metal-insulator transition occurs at 250 K in the analogous phase containing vanadium, namely, V_4O_7.[7] Structural studies showed that the transition is accompanied by a separation of charge into alternate chains of V^{3+} and V^{4+} sites running along the pseudorutile c axis. Both V^{3+} and V^{4+} sites show evidence for the formation of short bonds, but the maximum change in bond length at the transition is only 0.07 Å.[8]

Also, the next higher member of the vanadium series, V_5O_9, undergoes a single insulator-metal transition with decreasing temperature at ~135 K.[7] The crystal structures of both the metallic and insulating phases showed that in the former phase the charges are disordered, whereas in the latter one there are alternate chains of V^{4+} and predominantly V^{3+} sites running along the pseudorutile c axis.[9] However, no changes in metal-metal distances which exceeded 0.06 Å were observed at the transition. In the case of Ti_4O_7 the Ti^{3+} sites move toward each other so that the Ti-Ti distance between pairs decreases about 0.20 Å. Similarly, in the case of VO_2 there is pairing with a decrease in the V-V distance of 0.23 Å.[10] In terms of a relationship between bond order and bond length these changes imply a doubling of the bond order in the insulating phase over that in the metallic phase.[11] For V_4O_7 one could argue that the amount of pairing increases in the insulating phase with decreasing temperature because there is evidence from measurements of the electrical resistivity, magnetic susceptibility, ^{51}V NMR, and structure that the transition is only slightly first order. The structure of the insulating phase of V_4O_7 was refined only 50 deg below the transition so that one could indeed observe larger changes than 0.07 Å at lower temperatures. In V_5O_9 the transition is strongly first order and therefore the previous argument is no longer valid. Since NMR results clearly show the existence of some singlet-metal-metal bonds it was speculated that many bonding patterns could exist in an insulating V_5O_9 crystal. The idealized structure of the M_nO_{2n-1} oxides can be thought of as chains of edge-sharing octahedra along the c_R axis which are n octahedra in length and are connected to adjacent chains of the other rutile sections either by face sharing in the a_R direction or edge sharing in the b_R one. Within an infinite edge-sharing chain in the b_Rc_R plane there is the possibility of many patterns of metal-metal bonds, not only along the pseudorutile c_R axis in any one section of the chain, but also between chains. *A priori* there is no reason to expect one particular bonding pattern to predominate over the others and by classical x-ray diffraction methods an average of many different bonding patterns is observed. This would explain why in the insulating phase of V_5O_9 there is evidence only for the localization of charge, but not for the formation of metal-metal bonds.

This paper reports the determination of the crystal structure of Ti_5O_9 at room temperature, at 135 K, and at 120 K, along with electrical-conductivity, magnetic-susceptibility, heat-capacity, and electron-paramagnetic-resonance measurements. We thought that it would be of interest to extend such studies to an odd member of the titanium series.

II. EXPERIMENTAL

Single crystals of Ti_5O_9 were grown by the vapor-transport method by using Ti_4O_7 powder samples and $TeCl_4$ as the transporting agent. The Ti_4O_7 powders were prepared by reducing TiO_2 with purified H_2. The details of these preparations have been published elsewhere.[12] The impurity content of the Ti_5O_9 single crystals given by γ-ray activation analysis, is 20–400 ppm of Te, 20–200 ppm

of Cl, 20–30 ppm of Cr, and 1–4 ppm of Sc.

The conductivity between 77 K and room temperature was determined by the four-point technique which is commonly used for weak resistances. The low temperatures were attained by the use of a cryostat equipped with a temperature regulator.

The magnetic-susceptibilities measurements between 4 K and room temperature were performed with a vibrating-sample magnetometer (Foner type) equipped with a cryostat and a temperature regulator.

The transition enthalpies were determined with a differential scanning commercial calorimeter (Perkin-Elmer DSC 2) by comparison with the melting enthalpy of indium ($\Delta H = 6.8$ cal/g). The same apparatus was used for determining the specific heat between 115 K and room temperature. Benzoic acid was used as a reference standard.

The lattice parameters at room temperature were determined from a Guinier powder photograph taken with monochromatic Fe Kα radiation and using KCl as an internal standard. The lattice parameters as a function of temperature from 110 K to room temperature were determined from the single crystal which had been mounted on the diffractometer for the intensity data collection. The temperature of the crystal was controlled by blowing nitrogen gas at controlled temperatures over it. The least-squares refinement was applied on 20 reflections chosen in the region where a complete α_1/α_2 separation occurred. The zero of the ω circle was obtained by measuring the ω and $-\omega$ values for each reflection.

The x-ray intensity measurements for the three phases were taken at 298, 135, and 115 K with a computer-controlled, automatic, Philips, four-circle diffractometer, equipped with a Mo tube and a graphite monochromator. For the low-temperature measurements, the reflections, whose intensity and Bragg angle were very sensitive to the two transitions, were used as standard reflections and in the orientation matrix. This was very important for the data collection of the intermediate phase as its stability interval is only 10–12 deg. The specimen was a sphere 0.019 cm in diameter. The procedure for intensity data collection was the same for the three phases. All possible reflections in the region $2\theta < 80°$ were measured by the ω-scan technique. Before the integrated intensities of equivalent reflections were averaged a test was introduced in order to see whether the Friedel pairs had the same intensity. Since no differences between (hkl) and $(\overline{hkl})$ were observed within experimental limits, it was concluded that each phase of Ti_5O_9 was centrosymmetric. The Lorentz polarization and absorption corrections were applied. The total number of independent reflections with $I > 0$ was 5533, 5082, and 5104 for 298, 135, and 115 K, respectively. The structural refinements were carried out with the LINUS program together with the f curves for neutral atoms given by Doyle and Turner.[13] The real and imaginary anomalous correction coefficients for titanium were those given by Cromer and Liberman.[14] The positional and thermal parameters of V_5O_9 were used as the starting values.[9] The weighting scheme used has been described in detail elsewhere.[15] In the first few cycles the scale factor, the secondary extinction coefficient, 39 positional parameters, and 14 thermal isotropic parameters were varied. Anisotropic thermal coefficients were introduced in the final cycles of refinement. The conventional weighted R factors were 0.022, 0.027, and 0.025 for the structures at 298, 135, and 115 K, respectively. The final positional and thermal parameters for the three structures are listed in Tables I and II, respectively. The lists of observed and calculated structure factors are omitted, but are available on request. The interatomic distances and thermal data calculated by the program ORFFE for the room-temperature structure are reported in Tables III–V.

III. RESULTS

A. Lattice parameters

The lattice parameters are shown in Fig. 2 as a function of temperature. Two transitions are clearly observed which occur within an interval of 10–20 K. The lower transition (~128 K) is marked by discontinuities in lattice parameters and by a resulting volume change of $(-0.10 \pm 0.02)\%$, the low-temperature phase being less dense. The upper transition (~140 K) is marked only by discontinuities in the lattice parameters. The volume change which occurs at this transition is smaller than the estimated error. These results are different from those reported for Ti_4O_7. Only one transition was observed in the lattice parameters of Ti_4O_7 which was accompanied by a volume change of 0.04%.[3]

B. Electrical conductivity

Figure 3 shows the variation as a function of temperature of the conductivity of a single crystal of Ti_5O_9 from 77 K to room temperature. It can be seen that two distinct transitions take place, the first at ~128 K and the second, at 139 K. The conductivity decreases over all by a factor of 3, which is much smaller than the factor of 50 reported by Bartholomew and Frankl.[1] The discrepancy might be due to the different nature of the impurities present in the crystals. In agreement with the previous measurements[1] we found that the conductivity

TABLE I. Positional parameters.

		295 K	135 K	115 K
Ti(1)	x	0.0	0.0	0.0
	y	0.5	0.5	0.5
	z	0.0	0.0	0.0
Ti(2)	x	0.0	0.0	0.0
	y	0.0	0.0	0.0
	z	0.0	0.0	0.0
Ti(3)	x	0.553 56(5)	0.554 49(7)	0.555 17(6)
	y	0.843 93(4)	0.845 26(6)	0.845 26(5)
	z	0.206 36(3)	0.207 50(4)	0.207 16(4)
Ti(4)	x	0.552 21(5)	0.549 56(7)	0.549 76(6)
	y	0.344 28(4)	0.343 47(5)	0.343 49(5)
	z	0.205 15(3)	0.204 42(4)	0.205 00(4)
Ti(5)	x	0.140 36(5)	0.138 84(7)	0.137 74(6)
	y	0.173 51(4)	0.174 13(5)	0.174 09(5)
	z	0.421 33(3)	0.421 83(4)	0.421 16(4)
Ti(6)	x	0.147 91(5)	0.146 89(7)	0.147 00(6)
	y	0.675 37(4)	0.674 83(5)	0.674 47(5)
	z	0.423 86(3)	0.423 25(4)	0.422 33(4)
O(1)	x	0.6464(2)	0.6445(3)	0.6451(2)
	y	0.8519(1)	0.8519(2)	0.8517(2)
	z	0.0207(1)	0.0207(2)	0.0210(1)
O(2)	x	0.1628(2)	0.1621(2)	0.1613(2)
	y	0.8022(1)	0.8016(2)	0.8016(2)
	z	0.0805(1)	0.0801(1)	0.0796(1)
O(3)	x	0.3952(2)	0.3948(2)	0.3940(2)
	y	0.5382(1)	0.5379(2)	0.5369(2)
	z	0.1351(1)	0.1346(1)	0.1345(1)
O(4)	x	0.9218(2)	0.9212(2)	0.9217(2)
	y	0.4888(1)	0.4884(2)	0.4882(2)
	z	0.2034(1)	0.2026(1)	0.2023(1)
O(5)	x	0.2177(2)	0.2166(3)	0.2161(2)
	y	0.1918(1)	0.1923(2)	0.1918(2)
	z	0.2381(1)	0.2381(1)	0.2377(1)
O(6)	x	0.7314(2)	0.7289(2)	0.7281(2)
	y	0.1534(1)	0.1535(2)	0.1540(2)
	z	0.3240(1)	0.3237(1)	0.3238(1)
O(7)	x	0.9525(2)	0.9529(2)	0.9538(2)
	y	0.8673(1)	0.8667(2)	0.8660(2)
	z	0.3674(1)	0.3676(1)	0.3686(1)
O(8)	x	0.4906(2)	0.4905(2)	0.4905(2)
	y	0.8051(1)	0.8051(2)	0.8047(1)
	z	0.4195(1)	0.4190(1)	0.4186(1)
O(9)	x	0.7697(2)	0.7678(2)	0.7678(2)
	y	0.5306(1)	0.5287(2)	0.5283(2)
	z	0.4580(1)	0.4571(1)	0.4575(1)

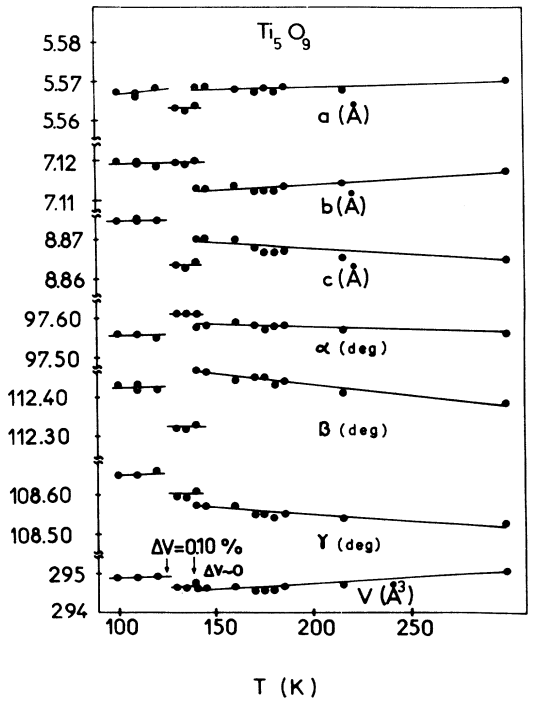

FIG. 2. Lattice parameters and unit cell vs temperature for Ti_5O_9.

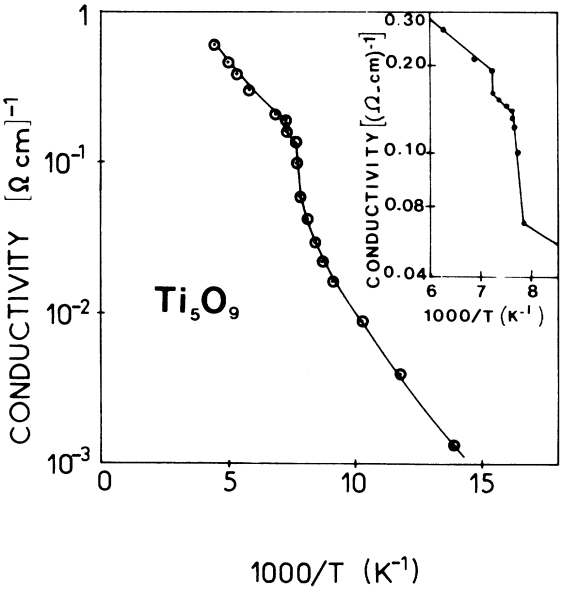

FIG. 3. Electrical conductivity vs temperature for a single crystal of Ti_5O_9.

TABLE II. Anisotropic temperature factors.

		298 K	135 K	115 K			298 K	135 K	115 K
Ti(1)	β_{11}	71.7(9)	65.0(1.3)	91.1(1.2)	O(3)	β_{11}	60(2)	46(3)	49(2)
	β_{22}	31.5(5)	30.9(8)	35.6(7)		β_{22}	28(1)	22(1)	21(1)
	β_{33}	27.1(3)	21.7(5)	18.4(4)		β_{33}	27(1)	16(1)	17(1)
	β_{12}	21.3(5)	28.6(8)	41.7(8)		β_{12}	21(1)	17(2)	15(1)
	β_{13}	16.4(4)	19.0(6)	19.1(6)		β_{13}	13(1)	10(1)	9(1)
	β_{23}	7.9(3)	14.4(5)	12.1(4)		β_{23}	9(1)	8(1)	8(1)
Ti(2)	β_{11}	61.8(8)	42.2(1.1)	47.7(1.0)					
	β_{22}	29.5(5)	21.2(7)	17.6(6)	O(4)	β_{11}	66(2)	47(3)	58(3)
	β_{33}	22.1(3)	11.7(4)	11.3(4)		β_{22}	36(1)	23(2)	22(1)
	β_{12}	19.2(5)	15.7(7)	13.9(6)		β_{33}	19(1)	13(1)	13(1)
	β_{13}	15.1(4)	9.1(5)	8.2(5)		β_{12}	12(1)	10(2)	12(2)
	β_{23}	7.7(3)	7.2(4)	4.6(4)		β_{13}	15(1)	10(1)	8(1)
						β_{23}	5(1)	5(1)	4(1)
Ti(3)	β_{11}	60.9(6)	48.4(8)	67.2(8)					
	β_{22}	29.1(3)	20.2(5)	19.0(4)					
	β_{33}	19.7(2)	12.4(3)	14.8(3)	O(5)	β_{11}	86(2)	58(3)	59(3)
	β_{12}	18.3(3)	15.9(5)	19.3(5)		β_{22}	41(1)	31(2)	28(1)
	β_{13}	13.5(3)	11.6(4)	17.2(4)		β_{33}	22(1)	12(1)	16(1)
	β_{23}	7.2(2)	6.8(3)	7.0(3)		β_{12}	23(1)	15(2)	17(2)
						β_{13}	23(1)	10(1)	14(1)
Ti(4)	β_{11}	59.5(6)	38.7(8)	43.0(7)		β_{23}	10(1)	7(1)	8(1)
	β_{22}	28.6(3)	19.6(5)	20.8(4)					
	β_{33}	20.8(2)	10.8(3)	12.9(3)					
	β_{12}	16.8(3)	12.4(5)	14.6(4)	O(6)	β_{11}	61(2)	47(3)	51(2)
	β_{13}	12.8(3)	6.2(4)	8.3(4)		β_{22}	28(1)	25(2)	24(1)
	β_{23}	6.1(2)	4.8(3)	6.1(3)		β_{33}	22(1)	15(1)	14(1)
						β_{12}	17(1)	15(2)	12(2)
Ti(5)	β_{11}	64.0(6)	52.5(8)	60.2(8)		β_{13}	13(1)	10(1)	10(1)
	β_{22}	27.4(3)	20.1(5)	17.9(4)		β_{23}	8(1)	9(1)	5(1)
	β_{33}	20.2(2)	15.4(3)	15.0(3)					
	β_{12}	19.2(3)	17.2(5)	16.2(4)					
	β_{13}	17.0(3)	13.2(4)	14.2(4)	O(7)	β_{11}	58(2)	44(3)	48(2)
	β_{23}	7.6(3)	8.9(3)	6.6(3)		β_{22}	29(1)	23(2)	25(1)
						β_{33}	20(1)	13(1)	14(1)
Ti(6)	β_{11}	58.7(6)	41.8(8)	49.2(7)		β_{12}	18(1)	13(2)	11(2)
	β_{22}	27.9(3)	18.3(6)	18.3(4)		β_{13}	13(1)	10(1)	10(1)
	β_{33}	23.2(2)	12.3(3)	14.9(3)		β_{23}	7(1)	7(1)	6(1)
	β_{12}	18.6(3)	10.5(5)	11.9(4)					
	β_{13}	15.4(3)	4.2(4)	4.0(3)					
	β_{23}	8.6(2)	5.1(3)	5.2(3)	O(8)	β_{11}	58(2)	39(3)	48(2)
						β_{22}	39(1)	24(2)	25(1)
O(1)	β_{11}	76(2)	57(3)	60(3)		β_{33}	21(1)	13(1)	14(1)
	β_{22}	40(1)	27(2)	27(2)		β_{12}	19(1)	11(2)	12(2)
	β_{33}	26(1)	18(1)	22(1)		β_{13}	15(1)	8(1)	10(1)
	β_{12}	18(1)	16(2)	16(2)		β_{23}	10(1)	8(1)	6(1)
	β_{13}	24(1)	15(1)	15(1)					
	β_{23}	9(1)	10(1)	10(1)					
O(2)	β_{11}	66(2)	51(3)	50(3)	O(9)	β_{11}	64(2)	49(3)	55(3)
	β_{22}	29(1)	19(1)	19(1)		β_{22}	27(1)	22(1)	23(1)
	β_{33}	31(1)	17(1)	19(1)		β_{33}	19(1)	13(1)	15(1)
	β_{12}	21(1)	14(2)	12(1)		β_{12}	16(1)	16(2)	15(2)
	β_{13}	15(1)	10(1)	10(1)		β_{13}	12(1)	8(1)	7(1)
	β_{23}	10(1)	7(1)	5(1)		β_{23}	6(1)	7(1)	6(1)

TABLE III. Interatomic distances (Å) in Ti octahedra for the room-temperature structure.

Ti(1)-O(2) ×2	1.9543(9)
-O(3) ×2	1.9666(9)
-O(4) ×2	2.0164(11)
Average	1.979
O(2)-O(3) ×2	2.598(2)
O(2)-O(3) ×2	2.937(1)
O(2)-O(4) ×2	2.797(1)
O(2)-O(4) ×2	2.819(1)
O(3)-O(4) ×2	2.780(1)
O(3)-O(4) ×2	2.853(2)
Average	2.787
Ti(2)-O(1) ×2	2.0090(11)
-O(2) ×2	1.9733(11)
-O(5) ×2	2.0044(8)
Average	1.996
O(1)-O(2) ×2	2.765(2)
O(1)-O(2) ×2	2.865(2)
O(1)-O(5) ×2	2.690(2)
O(1)-O(5) ×2	2.979(1)
O(2)-O(5) ×2	2.802(1)
O(2)-O(5) ×2	2.824(1)
Average	2.820
Ti(3)-O(1)	1.9073(12)
-O(2)	1.9264(10)
-O(3)	1.9756(9)
-O(6)	2.0342(9)
-O(7)	2.0673(9)
-O(8)	2.0866(11)
Average	2.000
O(3)-O(1)	2.769(2)
O(3)-O(2)	2.598(2)
O(3)-O(7)	2.928(1)
O(3)-O(8)	2.705(1)
O(6)-O(1)	2.986(2)
O(6)-O(7)	2.693(2)
O(6)-O(8)	2.824(1)
O(1)-O(2)	2.866(2)
O(1)-O(7)	2.852(1)
O(8)-O(2)	2.849(1)
O(8)-O(7)	2.697(2)
Average	2.817
Ti(4)-O(1)	1.9406(9)
-O(3)	1.9060(11)
-O(4)	1.9953(11)
-O(5)	1.9887(12)
-O(6)	2.0937(11)
-O(9)	2.0893(8)
Average	2.002
O(1)-O(3)	2.830(1)
O(1)-O(4)	2.979(1)
O(1)-O(5)	2.690(2)
O(1)-O(6)	2.959(1)
O(9)-O(3)	2.843(1)
O(9)-O(4)	2.712(2)
O(9)-O(5)	2.920(1)
O(9)-O(6)	2.696(1)
O(4)-O(3)	2.907(2)
O(4)-O(6)	2.810(1)
O(5)-O(3)	2.763(1)
O(5)-O(6)	2.780(2)
Average	2.824
Ti(5)-O(5)	1.8425(12)
-O(6)	2.0517(10)
-O(7)	1.9915(9)
-O(8)	1.9394(9)
-O(9)	2.0384(10)
Average	2.003
O(9)-O(5)	3.087(2)
O(9)-O(6)	2.698(1)
O(9)-O(7)	2.648(1)
O(9)-O(8)	2.838(2)
O(7)-O(5)	2.942(2)
O(7)-O(6)	2.681(1)
O(7)-O(7)	2.573(1)
O(7)-O(8)	2.895(1)
O(7)-O(8)	2.697(2)
O(7)-O(6)	2.693(2)
O(5)-O(8)	2.833(1)
O(5)-O(6)	3.027(2)
Average	2.801
Ti(6)-O(4)	1.8803(8)
-O(6)	2.1314(10)
-O(7)	2.0027(11)
-O(8)	1.8563(11)
-O(9)	1.9799(11)
-O(9)	2.1878(11)
Average	2.006
O(4)-O(7)	2.809(1)
O(4)-O(8)	2.908(1)
O(4)-O(9)	2.712(2)
O(4)-O(9)	2.878(1)
O(6)-O(7)	2.681(1)
O(6)-O(8)	3.000(2)
O(6)-O(9)	2.696(1)
O(6)-O(9)	2.698(1)
O(8)-O(7)	3.039(2)
O(8)-O(9)	2.947(2)
O(9)-O(7)	2.648(1)
O(9)-O(9)	2.581(1)
Average	2.800

TABLE IV. Ti-Ti distances (Å) for the room-temperature structure.[a]

Ti(1)-Ti(4) *c* ×2	3.5225(4)
-Ti(4) *c* ×2	3.6078(4)
-Ti(6) *c* ×2	3.4774(4)
-Ti(2) *c* ×2	3.5590(2)
-Ti(3) *e* ×2	2.9234(4)
Ti(2)-Ti(3) *c* ×2	3.5324(4)
-Ti(3) *c* ×2	3.6109(4)
-Ti(1) *c* ×2	3.5590(2)
-Ti(5) *c* ×2	3.4668(3)
-Ti(4) *e* ×2	2.9191(4)
Ti(3)-Ti(6) *c*	3.5349(5)
-Ti(6) *c*	3.7894(5)
-Ti(4) *c*	3.4660(4)
-Ti(4) *c*	3.5527(5)
-Ti(4) *c*	3.5653(5)
-Ti(1) *e*	2.9234(4)
-Ti(2) *c*	3.5324(4)
-Ti(2) *c*	3.6109(4)
-Ti(5) *e*	2.9988(4)
-Ti(6) *cb*	3.8036(5)
-Ti(5) *eb*	3.1210(4)
Ti(4)-Ti(3) *c*	3.4660(4)
-Ti(3) *c*	3.5527(5)
-Ti(3) *c*	3.5653(5)
-Ti(5) *c*	3.5540(5)
-Ti(5) *c*	3.7704(5)
-Ti(1) *c*	3.5225(4)
-Ti(1) *c*	3.6078(4)
-Ti(2) *e*	2.9191(4)
-Ti(6) *e*	3.0362(4)
-Ti(5) *cb*	3.8210(5)
-Ti(6) *eb*	3.1114(4)
Ti(5)-Ti(6) *c*	3.5561(4)
-Ti(6) *c*	3.5622(4)
-Ti(3) *e*	2.9988(4)
-Ti(4) *c*	3.5540(5)
-Ti(4) *c*	3.7704(5)
-Ti(2) *c*	3.4668(3)
-Ti(6) *fb*	2.8323(5)
-Ti(5) *eb*	3.2586(6)
-Ti(6) *cb*	3.3900(5)
-Ti(4) *cb*	3.8210(5)
-Ti(3) *eb*	3.1210(4)
Ti(6)-Ti(5) *c*	3.5561(4)
-Ti(5) *c*	3.5622(4)
-Ti(4) *e*	3.0362(4)
-Ti(3) *c*	3.5349(5)
-Ti(3) *c*	3.7894(5)
-Ti(1) *c*	3.4774(4)
-Ti(5) *fb*	2.8323(5)
-Ti(6) *eb*	3.2788(6)
-Ti(5) *cb*	3.3900(5)
-Ti(3) *cb*	3.8036(5)
-Ti(4) *eb*	3.1114(4)

[a] The symbols *c*, *e*, and *f* refer to Ti-Ti distances across a shared octahedral corner, edge, or face, respectively. The symbol *b* indicates Ti-Ti distances between rutile blocks.

TABLE V. Root-mean-square values for the room-temperature structure.

Ti(1)	1	0.0796(9)
	2	0.0881(4)
	3	0.0975(9)
Ti(2)	1	0.0766(9)
	2	0.0821(4)
	3	0.0865(9)
Ti(3)	1	0.0761(6)
	2	0.0787(3)
	3	0.0859(7)
Ti(4)	1	0.0773(4)
	2	0.0789(5)
	3	0.0849(7)
Ti(5)	1	0.0738(6)
	2	0.0783(6)
	3	0.0849(4)
Ti(6)	1	0.0735(7)
	2	0.0815(3)
	3	0.0867(7)
O(1)	1	0.083(3)
	2	0.091(1)
	3	0.099(2)
O(2)	1	0.073(3)
	2	0.086(1)
	3	0.104(2)
O(3)	1	0.072(3)
	2	0.085(1)
	3	0.101(2)
O(4)	1	0.077(1)
	2	0.085(2)
	3	0.098(2)
O(5)	1	0.079(5)
	2	0.094(1)
	3	0.099(2)
O(6)	1	0.075(3)
	2	0.080(1)
	3	0.092(3)
O(7)	1	0.076(2)
	2	0.079(1)
	3	0.085(3)
O(8)	1	0.079(1)
	2	0.082(2)
	3	0.092(3)
O(9)	1	0.076(1)
	2	0.078(2)
	3	0.090(3)

of Ti_5O_9 in the high-temperature phase increases with increasing temperature so that this oxide should not be considered a true metal.

C. Magnetic susceptibility

Figure 4 shows the variation as a function of temperature of the molar susceptibility (χ_m) for a single crystal of Ti_5O_9 from 225 to 4 K. There are two transitions which occur at 128 and 138 K, respectively. The first consists in an increase of a factor of 2 while the second consists in a drop of ~20%. These results are somewhat different from those reported by Danley and Mulay.[2] These authors reported only one transition in the susceptibility of Ti_5O_9. From the curve shown in Ref. 2, it seems that they missed the 137-K transition. Furthermore, Danley and Mulay reported that the susceptibility exhibited Curie-Weiss behavior both above and below the only transition.

The present measurements show a Curie behavior only at low temperature ($T < 40$ K). For $40 < T < 128$ K the temperature-independent susceptibility might be due to a Van Vleck paramagnetism as in other titanium oxides. Between 128 and 138 K it is difficult to determine whether or not the susceptibility is temperature independent as the temperature range is too small. In the high-temperature phase, one clearly observes temperature-independent behavior. It should be pointed out that from the point of view of the magnetic behavior Ti_5O_9 is quite different from Ti_4O_7: in the former compound there are two transitions, whereas in the latter only one has been observed.

D. Heat capacity

Figure 5 shows the variation of C_p vs T for a single crystal of Ti_5O_9. The curve shows two peaks, one centered at 142 K which is 6 K in width and a second centered at 131 K, 4 K in width. The enthalpies of the transitions are found to be 135 ± 5 and 110 ± 5 cal/mole, respectively. The corresponding entropy changes are 0.97 and 0.85 cal/mole K. These results show once again the difference between the two transitions which take place in Ti_4O_7 and those which take place in Ti_5O_9. In the former compound also two peaks were observed in the C_p-vs-T curve; however, the enthalpy changes were 468 ± 5 and 95 ± 5 cal/mole for the high- and low-temperature transition, respectively.

E. Crystal structures

In the structure of Ti_5O_9 there are six crystallographically-independent Ti atoms, two of which Ti(1) and Ti(2) are in special position, i.e., the center of symmetry. The two crystallographically-independent pseudorutile chains are formed by Ti(5)-Ti(3)-Ti(1)-Ti(3)-Ti(5) and Ti(6)-Ti(4)-Ti(2)-Ti(4)-Ti(6). These chains can be seen in Fig. 6. Ti_5O_9 represents the first member of the Ti_nO_{2n-1} homologous series in which there is at least one complete rutile unit cell, namely, those centered on Ti(1) and Ti(2).

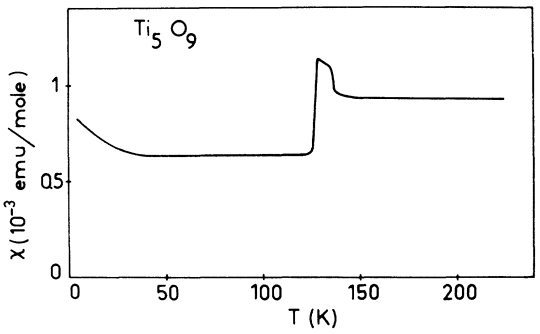

FIG. 4. Magnetic susceptibility vs temperature for a single crystal of Ti_5O_9.

At room temperature the average Ti-O distances are: for Ti(1)-O, 1.979; Ti(2)-O, 1.996; Ti(3)-O, 2.000; Ti(4)-O, 2.002; Ti(5)-O, 2.003; Ti(6)-O, 2.006 Å. The approximate electrostatic charges corresponding to these distances can be calculated from a plot of bond strength versus bond length (shown in Fig. 7) as discussed in Ref. 11. The values calculated for the six titanium atoms are reported in Table VI. Since Ti_5O_9 contains two Ti^{3+}

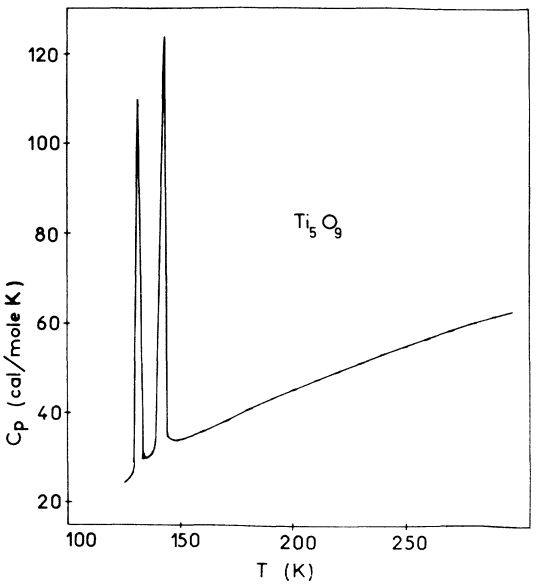

FIG. 5. Molar heat capacity C_p vs temperature for a single crystal of Ti_5O_9.

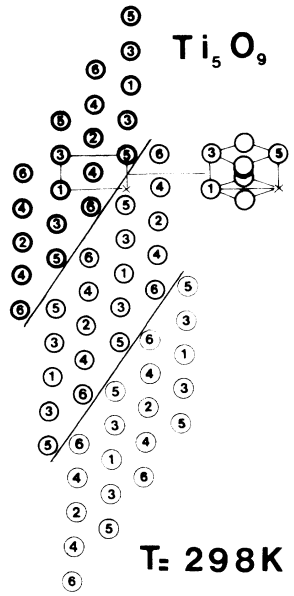

FIG. 6. Diagram showing the structure of Ti_5O_9. The sheets of cations (the anions are omitted for clarity) contain the pseudorutile directions [001] and [110] running vertically and horizontally, respectively. Each plane section is truncated by the shear planes as represented by the oblique lines while the different thicknesses of the circles indicate differences in the relative heights of each section. The inset shows the cation positions in rutile and defines the pseudorutile plane shown in the main figure. The numbers inside the circles designate the crystallographically inequivalent sites.

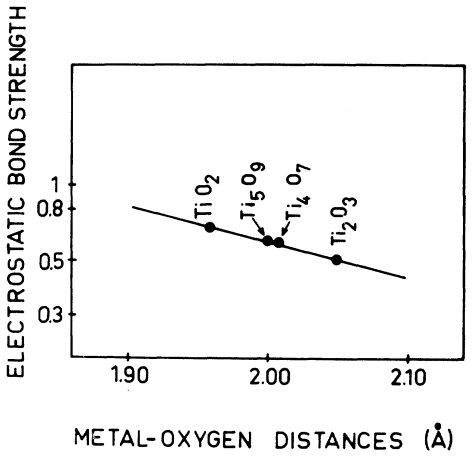

FIG. 7. Ti-O distances vs electrostatic bond strength. The experiment point are for valence states 3+, 3.5+, 3.6+, and 4+.

TABLE VI. Electrostatic charge on the titanium atoms.

	298 K	135 K	115 K
Ti(1)	3.85	3.91	3.92
Ti(2)	3.65	3.60	3.65
Ti(3)	3.60	3.60	3.56
Ti(4)	3.57	3.60	3.59
Ti(5)	3.56	3.52	3.50
Ti(6)	3.52	3.52	3.52
Average	3.60	3.60	3.59

and three Ti^{4+} cations the average charge on the titanium atoms should be 3.60. It can be seen from the values given in Table VI that the cationic charge is indeed uniformly distributed. However, as with Ti_4O_7, there are small individual deviations from the average. The atoms for which the surroundings resemble those of rutile to the greatest degree have a slightly larger charge, i.e., the sites well inside the rutile blocks are richer in 4+ cations whereas those toward the shear planes are richer in 3+ ones. An index of distortion of an oxygen polyhedron can be expressed as the standard deviation calculated from the average of the O-O distances. The values of this index, given in Table VII, increase on going from Ti(1) to Ti(5) along one pseudorutile chain and from Ti(2) to Ti(6), along the other one. Also, it seems that the pseudorutile 53135 chains, which have a larger separation of charge [Ti(1), 3.85+; Ti(5), 3.56+], are more distorted than the 64246 chains [Ti(2), 3.65+; Ti(6), 3.52+].

The Ti-Ti distance across the shared octahedral face, i.e., across the shear plane, Ti(5)-Ti(6), is 2.8323 Å which is slightly larger than the corresponding distance in Ti_4O_7 (2.811 Å). The Ti-Ti distances across the shared edges inside and between the rutile blocks vary from 2.9191 Å to 3.2788 Å which are typical of a metallic phase of a titanium oxide. In Ti_4O_7 the corresponding distances vary between 2.895 and 3.280 Å.

As it can be seen from Tables I and II and VI the structures of the low-temperature phases, one stable between 140 and 130 K and the other stable

TABLE VII. Index of distortion of the oxygen octahedra.

	298 K	135 K	115 K
Ti(1)	0.112	0.110	0.104
Ti(2)	0.097	0.096	0.093
Ti(3)	0.131	0.133	0.133
Ti(4)	0.101	0.100	0.100
Ti(5)	0.161	0.159	0.162
Ti(6)	0.151	0.148	0.149

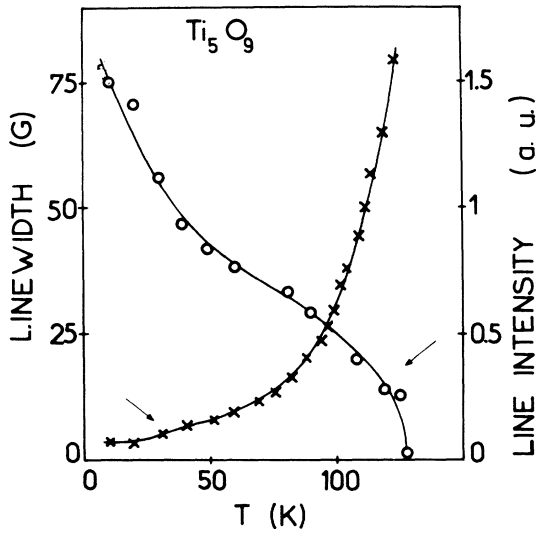

FIG. 8. Electron-paramagnetic-resonance data. Linewidth and integrated signal intensity vs temperature.

below 130 K are identical to the structure stable above 140 K. One does not observe in either one any localization of charges and/or formation of covalent bonds between the Ti^{3+} cations. This is in a way quite surprising as the localization of charges has been observed by classical x-ray diffraction methods in the insulating phases of Ti_4O_7, V_4O_7, and V_5O_9, the only exception being the intermediate phase of Ti_4O_7 for which a disordered model was proposed.

F. Electron paramagnetic resonance

Ti_5O_9 crystals show an intense EPR signal in the low-temperature phase. The g value is anisotropic and in the range of 1.94–1.98. Below 50 K the integrated intensity corresponds to a spin concentration of the order of 10^{21}–10^{22} spins/mole. Figure 8 shows the temperature dependence of the line width and of the intensity. While the linewidth is of the order of a few G at low temperature, it increases sharply just below the 130-K transition. At the same time, the intensity becomes vanishingly small. No EPR signal is detected in the intermediate phase. It is clear that the EPR line for $T < 130$ K has the same origin as the low-temperature Curie term of the susceptibility curve.

IV. DISCUSSION

The experimental data obtained for the three phases of Ti_5O_9 are summarized in Table VIII.

A. Low-temperature phase

The low-temperature phase is semiconducting; however, the x-ray data do not show any charge localization or pair bonding as in the low-temperature phase of Ti_4O_7. The magnetic susceptibility is temperature independent for $50 < T < 130$ K, but below 50 K it shows a large Curie term.

One may then propose the following model: charge localization occurs and Ti^{3+}-Ti^{3+} pair bonds are present in this phase. This would explain the semiconducting behavior as well as the Van Vleck temperature-independent paramagnetism. The

TABLE VIII. Properties of the three phases of Ti_5O_9 single crystals.

Temperature (K)	Low-temperature phase	~ 130 K	Intermediate phase	~ 140 K	High-temperature phase
Electrical conductivity	Semiconductor	Transition	Semiconductor	Transition	Semiconducting behavior (due to impurities?)
Magnetic susceptibility	Temperature-independent Van Vleck type	Transition		Transition	Temperature independent
Lattice parameters		Transition $\Delta V/V \simeq -0.1\%$		Transition $\Delta V/V \sim 0$	
Heat capacity		Transition $\Delta H = 110$ cal/mole $\Delta S = 0.85$ cal/mole K		Transition $\Delta H = 135$ cal/mole $\Delta S = 0.97$ cal/mole K	
Structure aspects		No transition		No transition	
EPR	Strong signal linewidth broadening	Vanishing of the signal			

Curie term would be due to a large proportion ($\sim 10^{-2}$) of unpaired Ti^{3+}. Such a large spin concentration cannot be due to magnetic impurities. Neither would it be likely that stoichiometry defects could be responsible for this behavior, as the deviation from stoichiometry for the Magnéli phases appears to be much smaller ($\sim 10^{-4}$). Therefore we suggest that the crystal contains microdomains and that the unpaired Ti^{3+} are mostly present at the domain walls. With such a domain structure it would not be possible to detect by the x-ray diffraction technique any charge localization and $Ti^{3+}-Ti^{3+}$ bond formation.

The EPR signal should be due to the unpaired Ti^{3+}; in fact the g value is consistent with a $3d^1$ configuration. The linewidth for $T < 20$ K should be due to dipolar coupling, while the large broadening below 130 K might be due to critical lattice fluctuations related to the approaching to the phase transition.

B. Intermediate phase

The vanishing of the EPR signal at 130 K seems to indicate that the microdomain structure disappears at this transition. The intermediate phase is also semiconducting and therefore it should contain $Ti^{3+}-Ti^{3+}$ bonds. We propose that this phase is a disordered phase as far as the $Ti^{3+}-Ti^{3+}$ pairs are concerned, just as the intermediate phase of Ti_4O_7.[6] Then the measured entropy at 130 K would have contributions due to disorder and lattice components. Such disorder cannot be detected by classical x-ray diffraction techniques. In the case of the intermediate phase of Ti_4O_7, the x-ray Debye-Waller thermal factors were anomalously large. The absence of such an effect in the intermediate phase of Ti_5O_9 could be due to the fact that the disorder is dynamic, with a lifetime smaller than $\sim 10^{-13}$ sec.

The magnetic susceptibility of this phase is also due to Van Vleck paramagnetism; the increase of χ at 130 K shows that the Ti_5O_9 band structure in this temperature range should be different from that of the low-temperature phase. Since the Van Vleck susceptibility is mainly due to the matrix elements between the singlet and triplet states of the Ti^{3+} pairs,[6] this result seems to indicate that the $Ti^{3+}-Ti^{3+}$ separation inside a pair should be larger in the intermediate than in the low-temperature phase.

C. High-temperature phase

From the specific-heat data one can readily see that Ti_5O_9 exhibits a second transition at 140 K. Above 140 K our crystals are still semiconducting and do not show any evidence of a metallic phase at high temperature. However, the conductivity of the high-temperature phase of flux-grown crystals was much higher than that of our crystals.[1] This difference might be due to different impurities in the two kinds of crystals.

The temperature-independent paramagnetism of the high-temperature phase could also be of Van Vleck type. The entropy change at the 140-K transition should then include a large lattice contribution.

ACKNOWLEDGMENTS

The authors wish to thank R. Buder for his valuable help in the susceptibility and EPR measurements and J. Mercier for his contribution in the crystal growth.

*Present address: Ecole-Mohammedia d'Ingenieurs, BP765, Agdal, Rabat, Marocco.

[1] R. F. Bartholemew and D. R. Frankl, Phys. Rev. 187, 828 (1969).
[2] W. J. Danley and L. N. Muley, Mater. Res. Bull. 7, 739 (1972).
[3] M. Marezio, D. B. McWhan, P. D. Dernier, and J. P. Remeika, J. Solid State Chem. 6, 213 (1973).
[4] P. W. Anderson, Mater. Res. Bull. 8, 153 (1973).
[5] C. Schlenker, S. Lakkis, J. M. D. Coey, and M. Marezio, Phys. Rev. Lett. 32, 1318 (1974).
[6] S. Lakkis, C. Schlenker, B.K. Chakraverty, R. Buder, and M. Marezio, Phys. Rev. B 15, 1429 (1976).
[7] H. Okinaka, K. Nagasawa, K. Kosuge, Y. Bando, S. Kachi, and T. Takada, J. Phys. Soc. Jpn. 32, 1148 (1972).
[8] M. Marezio, D. B. McWhan, P. D. Dernier, and J. P. Remeika, J. Solid State Chem. 6, 419 (1973).
[9] M. Marezio, P. D. Dernier, D. B. McWhan, and S. Kachi, J. Solid State Chem. 11, 301 (1974).
[10] J. M. Longo and P. Kierkegaard, Acta Chem. Scand. 24, 420 (1970).
[11] L. Pauling, *The Nature of the Chemical Bond* (Cornell U.P., Ithaca, 1960).
[12] J. Mercier and S. Lakkis, J.Cryst. Growth 20, 195 (1973).
[13] P. A. Doyle and P. S. Turner, Acta Crystallogr. A 24, 390 (1968).
[14] D. T. Cromer and D. Liberman, J. Chem. Phys. 53, 1891 (1970).
[15] J. Chenavas, J. C. Joubert, M. Marezio, and B. Bochu, J. Solid State Chem. 14, 25 (1975).